Electronic supplementary information

Point defect induced intervalley scattering for enhancement of interlayer electron transport in bilayer MoS₂ homojunction

Yang Ou[a], Zhuo Kang[a, b], Qingliang Liao[a, b], Shihan Gao[a], Zheng Zhang*[a,b] and Yue Zhang*[a,b]

a. Beijing Advanced Innovation Center for Materials Genome Engineering, Beijing Key Laboratory for Advanced Energy Materials and Technologies, University of Science and Technology Beijing, Beijing 100083, People's Republic of China.
b. State Key Laboratory for Advanced Metals and Materials, School of Materials Science and Engineering, University of Science and Technology Beijing, Beijing 100083, People's Republic of China.

* Corresponding Author: Prof. Yue Zhang Email: yuezhang@ustb.edu.cn,

Dr. Zheng Zhang Email: zhangzheng@ustb.edu.cn

S1 Bilayer MoS₂ band structure with spin orbital coupling

To evaluate the spin orbital coupling (SOC) effect in the interlayer transport, we also calculate the SOC band of monolayer/bilayer MoS₂ unit cell. The SOC of H-TMDC has already been proved by both theory [1] and experiment [2]. A schematic diagram of monolayer H-TMDC band structure is shown in figure R5(a). H-TMDC is a kind of multi-valley materials with K(K'), Q(Q') valleys in conduct band and K(K'), Γ valleys in valence band. The Γ valleys in valence band and K(K') valleys in conduct band are non-spin polarized while K(K') valleys in valence band and Q(Q') valleys in conduct band are spin polarized due to the strong SOC. Figure S1(b) represents the SOC band of monolayer MoS₂. The valence band K valleys band split by 0.15eV while conduct band Q valleys split by 0.07eV. We also find the CBM in K valley is 0.17eV lower than extrema of Q valley. To gather more information about the spin polarization, we also calculate the tilting angles (angle between spin direction and x-y plane) of valence band K(K') valley and conduct band Q(Q') valley. It is found that the spin flips when go from K(Q) to K'(Q'). In AB stacking bilayer MoS₂, the interlayer coupling modifies the band structure. A 0.6eV splitting appears in Γ valley, due to strong interlayer coupling. The splitting of valence band K valley is 0.16eV, only 0.01eV larger than that in monolayer. This is because in the weak interlayer coupling of these states and the top and bottom layers' opposite spin polarization. The localization degree of valence band K valley is extremely high, indicating the holes can hardly interlayer hopping through these states. Although the spin polarization of Q valley is also opposite between the two layers, but due to the strong interlayer coupling and small SOC splitting in monolayer Q(Q') valley, the splitting in conduct band Q valley is 0.36eV, 0.29eV bigger than that in monolayer. The Q valley states are interlayer mixed according to the LD (the bands are red near Q valley) The wave function in can be simply written by disturb theory.

$$| \psi_{n,k,s}^{t,b} \, ' \rangle = | \psi_{n,k,s}^{t,b} \rangle + \Delta \, | \psi_{n,k,s}^{t,b} \rangle = | \psi_{n,k,s}^{t,b} \rangle + \sum_m \frac{|t_{k,m,n,s}|^2}{E_{n,k,s} - E_{m,k,s}} | \varphi_{m,k,s}^{b,t} \rangle$$

Where $|\psi_{n,k,s}^{top}\rangle$ is the nth band at k point eigen sate of isolated top layer while $|\varphi_{m,k,s}^{bot}\rangle$ is the mth band at k point eigen sate of isolated top layer. $E_{n,k,s}$ and $E_{m,k,s}$ are energy level of n_{th} or m_{th} band at k point. $t_{k,m,n,s}$ is interlayer hopping integral. This equation implies that a small SOC splitting would not strongly suppress interlayer hopping in Q valley of bilayer MoS$_2$. We compare the DL in Q valley extrema of SOC and non-SOC band structure of bilayer MoS$_2$, the LD of SOC band is 0.06 while the that of non-SOC band is 0.0026. Like what happened in non-SOC result, the energy level of Q valley extrema in bilayer MoS2 is lowered to only 0.01eV higher than CBM in K valley. This result indicating the novel interlayer transporting of Q valley electrons in SOC AB stacking bilayer MoS$_2$. Considering the K-Q scattering does not demand spin flipping (unlike that in K-K' or Q-Q' scattering), our non-SOC result can qualitatively describe the K-Q scattering in condition with SOC.
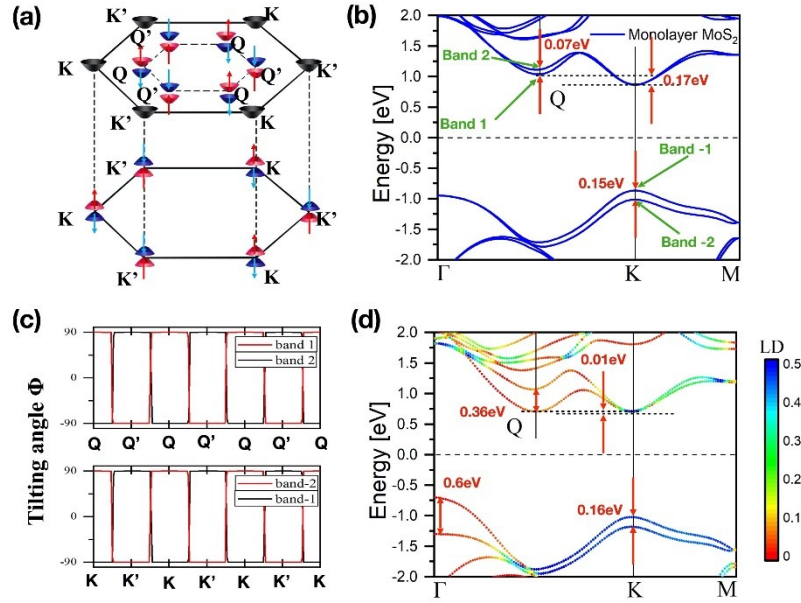

Figure S1 (a) schematic diagram of H-TMDC band structure. (b) calculated SOC band structure of monolayer MoS$_2$. (c) spin polarization direction tilting angles of K(K') and Q(Q') valley states. (d) calculated SOC band structure of AB stacking bilayer MoS$_2$.

S2 The interlayer distances

We measure both the S-S and Mo-Mo gap of each structure, as shown in figure S2. S-S gap is commonly seen in DFT works. Considering the band edge states are almost contributed by Mo orbitals, we also measured the Mo-Mo gap. Because there are many atoms in our structure (for pristine bilayer MoS$_2$, there are 432 atoms including 144 Mo and 288 S), so the result is exhibited by gap average and variance. The average gap is defined as $d_{el}=E(R_{el,up})-E(R_{el,bottom})$. Where $E(R_{el,up})$ and $E(R_{el,bottom})$ are average z coordinate of up and bottom layer el(iS or Mo) atoms (S-S or Mo-Mo). We roughly treat the position of up layer and bottom layer are independent, so the gap variance is defined as $D_{el}=D(R_{el,up})+D(R_{el,bottom})$. Where $D(R_{el,up})$ and $D(R_{el,bottom})$ are z coordinate variance. The results are shown in table S1. We sort in ascending sequence by d_{el}. For both S-S gap and Mo-Mo gap, the orders are iMo-S, V-Mo, Mo-S, V-S, iV-S, pristine for both S-S gap and Mo-Mo gap. Such result suggests the interlayer coupling in iMo-S is the strongest among all calculated structures. This can partly explain the largest improved in iMo-S.
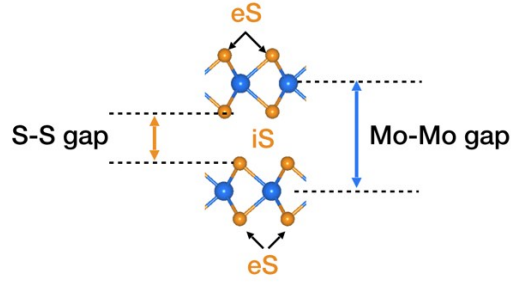
Figure S2 scheme of measuring interlayer distance.

Table S1 statistic results of interlayer distance.

Structure	E(S-S) [ang]	D(S-S) [ang^2]	E(Mo-Mo) [ang]	D(Mo-Mo) [ang^2]
V-S	3.1431	2.221^{-4}	6.2743	2.4614^{-4}
iV-S	3.1451	8.1475^{-5}	6.2774	1.7090^{-4}
Mo-S	3.1415	7.0270^{-4}	6.2728	8.4304^{-4}
iMo-S	3.1365	2.5073^{-4}	6.2704	5.3015^{-4}
V-Mo	3.1395	1.2277^{-4}	6.2712	1.0171^{-4}
Pristine	3.1544	0	6.2845	0

S3 Effective potential and potential deformation

Effective potential is important for understand the short-range scattering process.

We plot the x-y plane average effective potential ($V_{eff\_x\text{-}y}$) of each defective structure and then the y-z plane average effective potential difference ($\Delta V_{eff\_y\text{-}z}=V_{eff\_y\text{-}z}$(defective)-$V_{eff\_y\text{-}z}$(pristine)). Figure S3 (a)-(e) obviously show that the potential deformations are almost localized within a single unit cell which is highlighted by red frame. The V-S, iV-S and V-Mo increase the local potential (light green) while Mo-S and iMo-S decrease the local potential (dark blue).
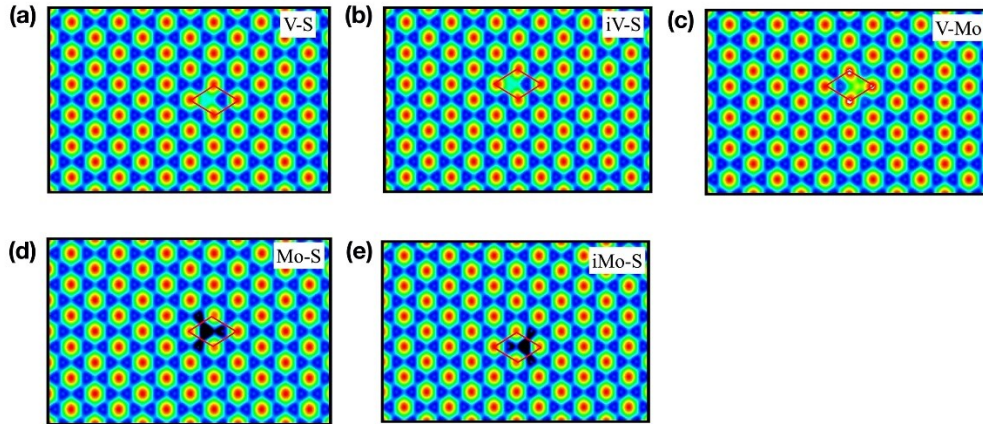

Figure S3 (a)-(e) are ($V_{eff\_x\text{-}y}$) potential of bilayer MoS$_2$ with V-S, iV-S, V-Mo, Mo-S and iMo-S.

We also plot the $\Delta V_{eff\_y\text{-}z}$ of each structure, as shown in figure S4. The $\Delta V_{eff\_y\text{-}z}$ confirm that the potential deformation mainly impacts the single layer with point defect. But the deformation also tinny influence the adjacent area. We can go further compare the magnitude of $\Delta V_{eff\_y\text{-}z}$ among these point defective structures. The extrema of $\Delta V_{eff\_y\text{-}z}$ in V-S, iV-S, V-Mo are about 0.07, 0.07 and 0.12 Hartree while the extrema of $\Delta V_{eff\_y\text{-}z}$ in Mo-S and iMo-S are about -0.077 and -0.09 Hartree respectively. The largest magnitude of $\Delta V_{eff\_y\text{-}z}$ partly explains the most efficient interlayer K-Q scattering in iMo-S.
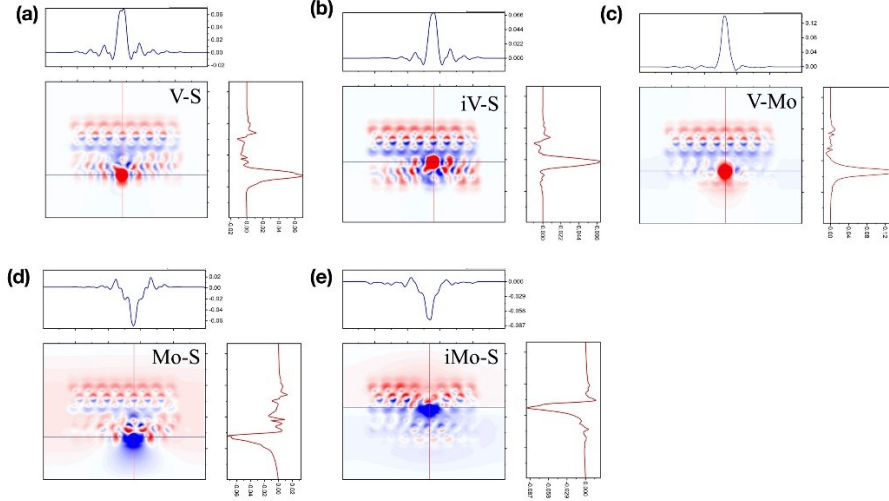

Figure S4 (a)-(e) ΔVeff_y-z of V-S, iV-S, Mo-S, iMo-S and V-Mo respectively.

Figure S5(a) reviews the figure 3g in main article, indicating a near 0.1eV splitting of K valley states in bilayer MoS_2 with point defect iMo-S. In order to confirm the originate of such splitting, we investigate the average effective potential along z axis (V_{eff_z}) of all defective and pristine structures. The calculated V_{eff_z} of pristine bilayer MoS_2 is shown in figure S5(b). To evaluate how point defect influence on the V_{eff_z}, we plot $\Delta V_{eff\_z} = V_{eff\_z}$ (defective)- V_{eff_z} (pristine) in figure R1(c). According to the V_{eff_z}, the 5 types of point defect, including V-S, iS-V, V-Mo, Mo-S and iMo-S, increasing the V_{eff_z} of the defect-free top layer. 4 in 5 point-defects increasing the V_{eff_z} of bottom layer, except iMo-S which remarkably lower the V_{eff_z} of bottom layer. Such V_{eff} difference between top and bottom layers generate the large splitting in figure S5(a).
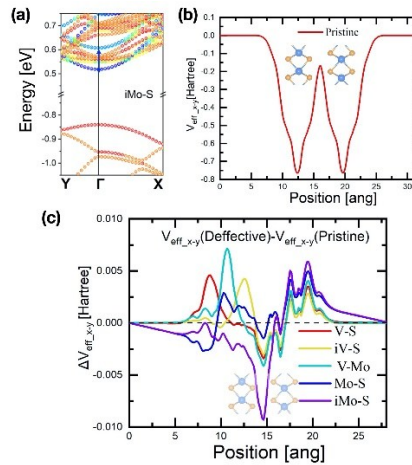

Figure S5 (a) repost of figure 3g in main article. (b) Veff_z of Pristine bilayer MoS_2. (c) ΔVeff_z of defective bilayer MoS_2 structures.

References

[1] Di Xiao, G. B. Liu, W. Feng, X. Xu, W. Yao, et al., Physical review letters, 2012, 108, 196802.

[2] H. Zeng, J. Dai, W. Yao, D. Xiao, X. Cui, Nature nanotechnology, 2012, 7, 490-493.